In situ transmission electron microscopy study of the crystallization of fast-growth doped SbxTe alloy films

Kooi, BJ; Pandian, R; De Hosson, JTM; Pauza, A

Published in:
Journal of materials research

DOI:
10.1557/JMR.2005.0228

Publication date:
2005

In situ transmission electron microscopy study of the crystallization of fast-growth doped Sb_xTe alloy films

Bart J. Kooi,[a] R. Pandian, and J.Th.M. De Hosson
Department of Applied Physics, Materials Science Centre and Netherlands Institute for Metals Research, University of Groningen, 9747 AG Groningen, The Netherlands

Andrew Pauza
Plasmon Data Systems Ltd., Hertsfordshire, SG8 6EN, United Kingdom

(Received 11 November 2004; accepted 15 March 2005)

Crystallization of amorphous thin films composed of doped Sb_xTe with $x = 3.0$, 3.6, and 4.2 and constant dopant level was studied by in situ heating in a transmission electron microscopy. Magnetron sputtering was used to deposit 20-nm-thick films sandwiched between two types of 3-nm-thick dielectric layers on 25-nm-thick silicon-nitride membranes. One type of dielectric layer consists of $ZnS–SiO_2$ (ZSO), the other of GeCrN (GCN). Crystallization was studied for temperatures in-between 150 and 190 °C. The type of dielectric layer turned out to strongly influence the crystallization process. Not only did the nucleation rate appear to depend sensitively on the dielectric layer type, but also the growth rate. The velocity of the crystalline/amorphous interface is about 5 times higher for the $x = 4.2$ film than for the $x = 3.0$ film if ZSO is used. In case of GCN, the interface velocity is about 2 times higher for the $x = 4.2$ film than for the $x = 3.0$ film. The activation energy for crystal growth is not significantly dependent on the Sb/Te ratio but is clearly different for ZSO and GCN—2.9 eV and 2.0 eV, respectively. The incubation time for the crystal nuclei formation is longer for ZSO than for GCN. Although the effects of the Sb/Te ratio and the dielectric layer type on the growth rates are strong, their effects on the nucleation rate are even more pronounced. A higher Sb/Te ratio results in a lower nucleation rate and the use of GCN instead of ZSO leads to higher nucleation rates.

I. INTRODUCTION

The crystallization rate in phase change optical recording, known from the rewritable CD and DVD formats, is becoming increasingly important because of the increasing demands on data-transfer rates. Crystallization is the rate-limiting process because amorphization is inherently a much faster process that in principle can be performed within femto-seconds.[1] $Ge_2Sb_2Te_5$ shows nucleation-dominated crystallization; i.e., it nucleates easily and fast, but it shows only limited growth, with final sizes of the crystallites within a disk of 10–30 nm.[2,3] With the ongoing decrease of the amorphous-mark sizes due to a decrease in laser wavelength and an increase in numerical aperture of the focusing lens, phase-change materials showing very fast growth (i.e., growth-dominated crystallization) tend to become more preferable than $Ge_2Sb_2Te_5$, at least with respect to attainable data-transfer rates.[3,4] If the bit size decreases, the distance a fast growing crystal has to proceed from the edge of the amorphous mark to its center decreases, and consequently the rewriting speed increases. For decreasing mark sizes, nucleation becomes less an issue since "nuclei" are always available at the edge of the mark. Therefore, phase-change materials show very low nucleation rates, but the fastest growth rates become increasingly important. Apart from application to optical recording, phase change materials are also of considerable interest for electrically based memory devices (nonvolatile solid state memories and scanning probe data storage) due to the large difference in resistivity (up to four orders in magnitude) for the amorphous and crystalline phase.

The fast-growth type of phase-change materials is investigated in the present work. These materials are based on a Sb-rich Sb-Te eutectic composition (Sb_xTe with $x = 3.0$, 3.6, and 4.2), since it is known that these Sb-rich alloys show highest crystallization rates.[3,4] A systematic study is made of the influence of these three different Sb/Te ratios on the crystallization kinetics, in particular

[a]Address all correspondence to this author.
e-mail: B.J.Kooi@rug.nl
DOI: 10.1557/JMR.2005.0228

the crystal growth rate. The "dopant" level (about 8 at.% In + Ge) is kept constant for these three ratios. In previous work, the strong effect of varying the Ge dopant level in $Sb_{3.6}Te$ was studied.[5] In addition, the present work addresses the influence of two types of thin dielectric layers between which the phase-change layer is sandwiched, on the crystallization kinetics.

The crystallization process is studied by transmission electron microscopy (TEM) using in situ heating. The advantage of this technique is that it provides detailed information with a high spatial resolution (nuclei with a size of 5 nm are detectable), allowing nucleation (rates) and growth (rates) to be monitored separately. Most techniques for the determination of crystallization kinetics measure the overall crystallization rate, which is an interplay of nucleation and growth, but are unable to unravel these separate contributions. Crystal structure(s), crystal size distributions, crystal shapes, crystal orientations, and defects within the crystals grown can be assessed using TEM. A disadvantage of TEM could be that the electron beam of the TEM affects the crystallization process. In a previous study on $Ge_2Sb_2Te_5$, the electron beam turned out to strongly enhance the nucleation rate, obscuring a normal (isothermal or isochronal) analysis of the transformation kinetics.[6] Similar effects were observed for $Sb_{3.6}Te$ (with different Ge concentrations), but when they were analyzed, it was found that the growth rates could still be measured reliably.[5]

II. EXPERIMENTAL

Magnetron sputtering was used to deposit 20-nm-thick doped Sb_xTe films sandwiched between 3-nm-thick amorphous dielectric layers. Three different values for the Sb/Te ratio were used ($x = 3.0$, 3.6 and 4.2), and sandwiching occurred between two types of dielectric layers. One dielectric layer type is based on 80 at.% ZnS–20 at.% SiO_2 (ZSO), the other on (Ge,Cr)N (GCN). The 'dopant' level (about 8 at.% In + Ge) is kept constant for the three Sb/Te ratios. As substrates for deposition commercially obtained (Agar Scientific, Stansted, Essex, UK) 25-nm-thick amorphous silicon-nitride membranes were used. Such electron-transparent substrates are obtained by etching $500 \times 500\ \mu m^2$ windows in a Si wafer containing a thin Si-nitride film on one side. The deposited samples could be directly analyzed (plan-view) with TEM; i.e., additional preparation steps were not needed.

Direct current (dc) sputtering with a power of 0.25 kW in argon with a pressure of 1.0 Pa was used to produce the phase-change layer. The target–sample distance was 31 mm. Radio frequency (rf) sputtering with a power of 0.8 kW in argon with a pressure of 0.75 Pa was used to obtain the ZSO dielectric layers. The GCN dielectric layers were obtained by rf sputtering with a power of 1.0 kW in an argon:nitrogen mixture of 2:1 with a pressure of 2.8 Pa. For both types of dielectric layers the target-sample distance was 43 mm. Targets for sputtering had a diameter of 200 mm.

For TEM, a JEOL 2010F operating at 200 kV was used. A Gatan (Pleasanton, CA) double tilt heating holder (model 652 with a model 901 SmartSet Hot Stage Controller) was used, which employs a Proportional Integral Derivative controller for accurate control of the temperature (within ±0.5 °C) and for a fast ramp rate to attain the desired final temperature without overshoot. Most in situ TEM studies suffer from a poor manual control of the temperature leading to significant scatter in data points e.g. with respect to nucleation and growth rates. Note that the temperature of the thin area that is imaged using TEM is generally lower than the nominal temperature indicated by the heating element within the specimen holder; i.e., the higher the temperature, the larger the discrepancy. Our work is performed below 200 °C, so the discrepancy will be on the order of only a few degrees. Nevertheless, for a correct comparison of the various samples, it turned out to be important to confine the measurements to a small area (always with the same dimensions) at the edge of the Si-nitride window. A clear gradient in number of crystal nuclei that develop and in their size due to subsequent growth was observed as a function of distance from the edge to the center of the window. Within the relatively small analysis area, this gradient is irrelevant.

To measure the crystal growth rates accurately, crystallization is monitored at relatively high magnifications (100,000×) within the TEM. This has two main disadvantages. First, the number of nuclei that develop in the observed area is very low (say 4 to even below 1), preventing a statistical accurate analysis of the nucleation rate. However, this is not a serious disadvantage, since previous work showed that the electron beam of the TEM clearly increased the nucleation rate, which, therefore, should not be analyzed by continuous monitoring at the transformation temperature but after cooling down to room temperature and analyzing areas that were not exposed to the electron beam at elevated temperature.[5,6] Second, the higher the magnification, the higher the current density of the electron beam of the TEM that is transmitted through the sample. This increases the possible influence of the electron beam on nucleation and growth. Previous work showed that the influence on nucleation was large but not significant on growth.[5] In the present work, however, the electron beam also clearly increased the crystal-growth rate. This difference between the present and the previous work is likely to be a consequence of using sputtered films in this study versus electron-beam evaporated films in the previous one.[5] More details on this difference are presented within the results below (Sec. III. B). To analyze the effect of the activation by temperature, care was taken to always use

an identical current density of the electron beam through the sample. Nucleation and growth can of course also be measured by intermittent heating within the TEM (without observation) and cooling to room temperature where the observations takes place. Results of such a study including a comparison of the growth rates obtained with and without electron-beam exposure will be given in a separate paper.[7]

III. RESULTS AND DISUSSION

A. In situ TEM observations of crystal growth

Reasonable incubation times for crystallization (within 1 h) and absence of crystallization before the desired isothermal transformation temperatures is reached put clear bounds on the temperature interval that is suitable for the (in situ TEM) study of crystallization. For the alloy films presently addressed, this temperature interval turned out to be between 150 and 190 °C (i.e., reading of the furnace thermocouple, where the actual analyzed area will be consistently a few degrees lower in temperature). The incubation time for crystallization appeared to be clearly shorter when the dielectric layers GCN were used instead of ZSO. Therefore crystallization of the phase-change films sandwiched between GCN was possible starting at about 150 °C, whereas for sandwiching between ZSO, it was possible starting at about 160 °C.

An example of the results of in situ TEM monitoring of the crystallization is shown in Fig. 1; this specific example holds for an Sb/Te ratio of 3.0, ZSO dielectric layers, and an isothermal transformation temperature of 170 °C. The incubation time in this case was about 4.5 min (starting when the temperature reached 169 °C). The images show that the growing crystals are more or less circular, so growth is generally isotropic. Clearly anisotropic growth was observed in previous work on undoped $Sb_{3.6}Te$, where intermediate dopant level (5 at.% Ge) clearly decreased the anisotropy.[5] When the

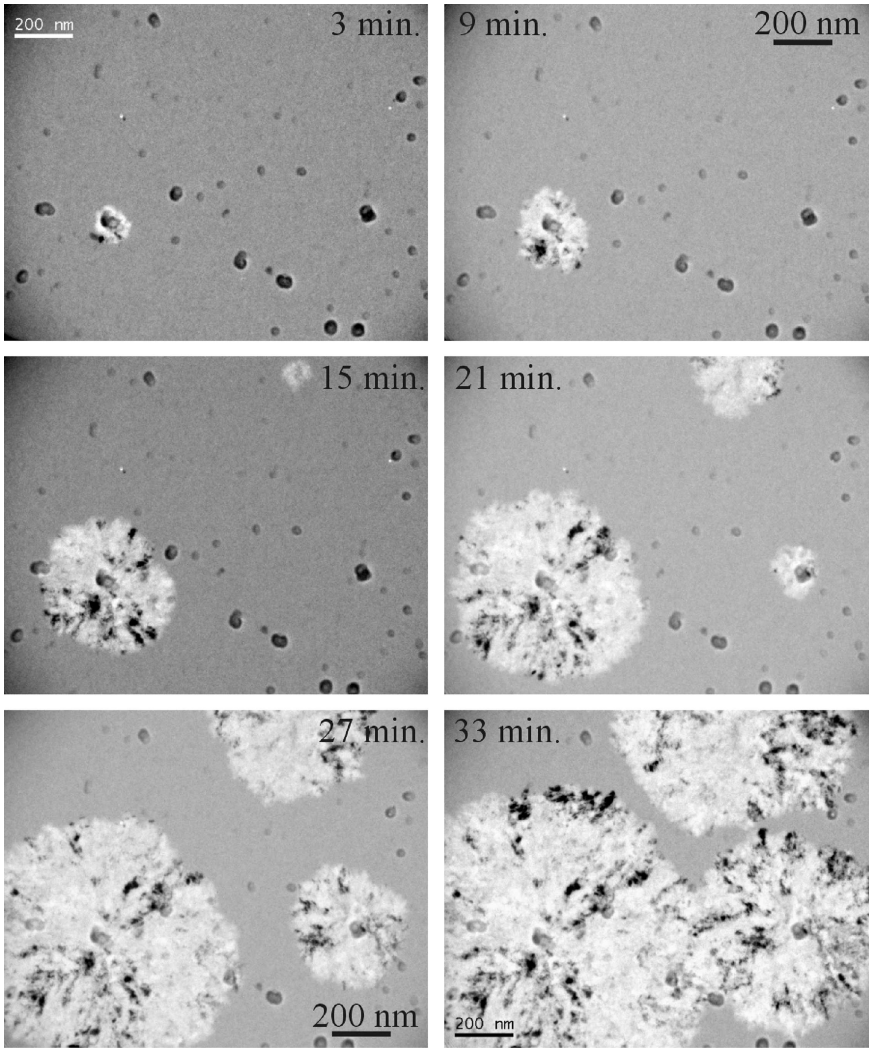

FIG. 1. Bright-field TEM images of crystal growth during heating at 170 °C of a phase-change film with an Sb/Te ratio of 3.0 sandwiched between $ZnS–SiO_2$. The time indicated in the images is the time used for growth after the incubation time has passed, which for this example was 4.5 min.

dielectric layers were GCN, growth appeared to be slightly less isotropic than ZSO.

Images of the as-deposited amorphous film show the presence of distinct particles with a size up to 40 nm. Later on we detected that a nonuniform thickness of the commercially obtained Si-nitride windows was partly responsible for the "particle" contrast as we checked on as-received windows. However, also nano-clusters were detected by TEM (see e.g., Fig. 1) and tapping mode AFM. These clusters were observed for the three types of Sb/Te ratios and the two types of dielectric layers. Energy-dispersive x-ray spectrometry (EDX) measurements connected to the TEM indicated that these particles appear to be slightly enriched in GeTe (and depleted in Sb). They probably developed because multiple targets were used for sputtering to arrive at the films with the large variation in Sb/Te ratio. Indeed, subsequent work on phase-change films sputtered from a single target showed that these particles were then absent. During the sputter process in the gas/plasma phase, atoms from the different targets apparently aggregate and form clusters that are subsequently deposited. Chemical bonding preferences (e.g., between Ge and Te) during this aggregation can maybe explain the composition of the clusters that then slightly deviates from the average one of the phase change layer. These clusters had clear influence on nucleation; they appeared preferential sites for nucleation. Nevertheless, significant differences in nucleation rate were still observed for the various Sb/Te ratios and the two dielectric layer types as will be discussed below (Sec. III. D). Moreover, the overall growth rates within the films measured were not affected by the presence of these particles. Since the thickness of the phase change layer is controlled by the mass change, the presence of the clusters reduced the thickness of the phase change film. However, from the particle density and their size, it can be estimated accurately that the film thickness was not smaller than 18 nm instead of the nominal 20 nm. The effect of the particles on the nominal composition of the phase-change layer was negligible. Differences in chemical composition between the crystalline and amorphous phases were not detected by TEM-EDX using a nano-probe. Also, directly after nucleation around the nano-clusters, the composition in the phase-change film in both the amorphous and crystalline phases was uniform. Therefore, the growth is definitely not diffusion controlled and must be interface controlled.

The crystals, as depicted in the bright-field TEM images, are generally brighter than the surrounding amorphous matrix. This shows that the crystals are not viewed along a low index crystallographic direction (where substantial diffraction would cause a strong reduction of the intensity of the undiffracted beam). It also shows that the crystal structure does not have a high density (per unit of solid angle) of low index directions as would be the case for e.g. an face-centered cubic (fcc) based structure. Selected-area electron diffraction (SAED) patterns indicate that the present structure is $R\bar{3}m$ with $a = 0.43$ nm and $c = 1.13$ nm, which is isomorphic with pure Sb. This was already revealed in our earlier work on $Sb_{3.6}Te$.[5] Within the bright crystals, dark/black lines can be discerned [particularly clear in Fig. 6(b) below]. This observed contrast shows that within each nucleated and grown crystal, bending of crystal planes occurs. This bending was more easily, directly and unambiguously observed in our work on $Sb_{3.6}Te$[5] because there each crystal nucleated preferentially with the [0001] crystal directions perpendicular to the surface. During subsequent growth, bending away from this initial orientation was apparent (where the amount of bending could be quantified). Here, this strong preference for a certain nucleus orientation is absent. This clear difference with previous work can probably be understood, because previously, the phase change films were uncapped, and to minimize the surface energy, a nucleus developed with its (0001) plane parallel to the surface. Now, due to the presence of the dielectric layer on top of the phase-change layer or of the nano-particles, nucleation apparently does not require this initial orientation. However, from the image contrast, it can still be deduced that bending remains to play a significant role. However, the amount of bending cannot be quantified anymore. It seems that the amount of bending is reduced if capping occurs. In light of the model proposed in Ref. 5 for the origin of this bending (i.e., why trans-rotational crystals develop), it is logical that capping has a substantial influence on the amount of bending. In the previous work, each nucleated crystal could still be called a single crystal (although severely bent and therefore better be called a trans-rotational crystal[8]). In the present work, due to the capping, a crystal splits up during growth in domains with less correlated orientations than in a trans-rotational crystal, in agreement with the polycrystalline diffraction patterns observed.

B. Crystal growth velocities influenced by relaxations

A larger number of images than shown in Fig. 1 allow the measurement of the average crystal diameter as function time. The result is shown in Fig. 2(a). The slopes of the linear regressions in Fig. 2(a) allow the determination of the crystal growth velocities (i.e., half of the values of the slope because they correspond to the advancement of two interfaces). Two systematic effects are observable in Fig. 2(a). First, the crystal size is generally not a linear function of time, but the growth rate increases with time. To observe this, the number of data points has to be sufficiently large and the time interval sufficiently long.

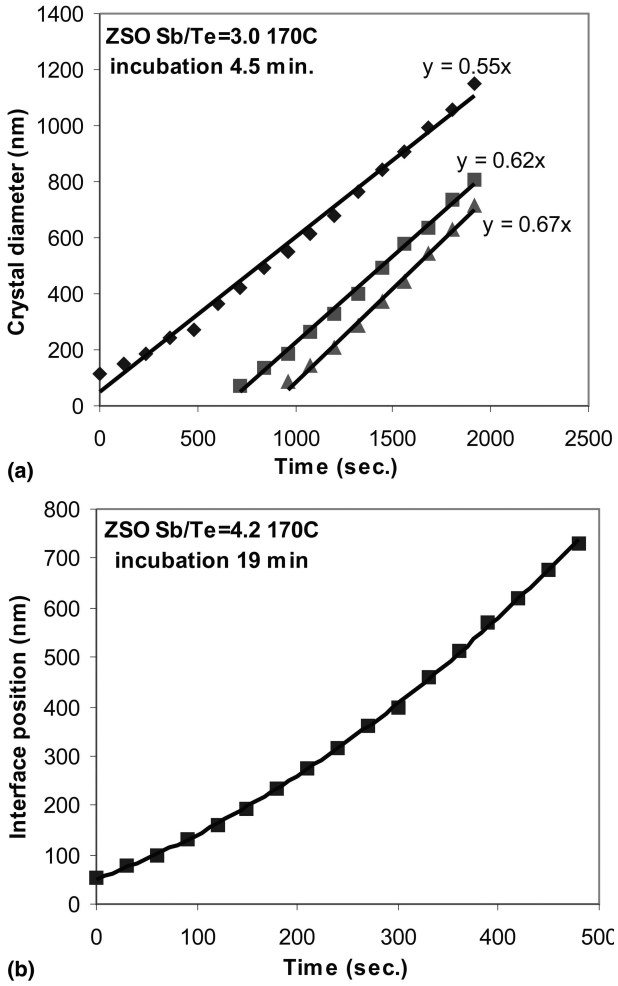

FIG. 2. From the change of the crystal diameter or the interface position (corrected for drift) as a function of time, the crystal growth rate can be obtained. The growth rate is not constant but appears to increase proportional with time. The crystal growth shown in Fig. 1 is the basis for the results shown in (a).

Therefore, this effect was probably not detected in previous growth studies on sputtered phase-change films.[9–12] Figure 2(b) shows another example of the deviation from linear growth. It turns out that the positive curvature can be accurately described by a parabolic fit. This shows that the increase of the growth velocity is approximately a linear function of time. The second connected effect is that crystals that nucleate later show on average a higher growth velocity. This is observable in Fig. 2(a), and another example is shown in Fig. 3. For the case shown in Fig. 3, crystallization of the observed area occurred within the order of a few minutes and therefore a difference of incubation time clearly longer than this crystallization time resulted in a clear difference in growth velocity. The growth velocities between 4 and 6 nm/s hold for a short incubation time of 2 min., whereas the growth rates between 10 and 11 nm/s hold for an incubation time of 10 min.

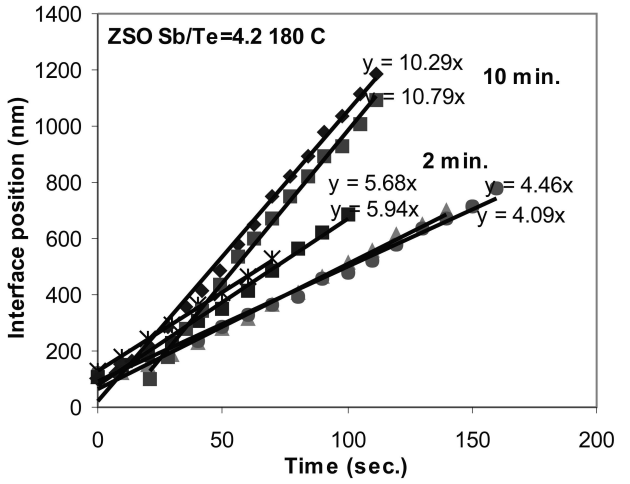

FIG. 3. Interface positions (corrected for drift) as a function of time during crystallization of a film with an Sb/Te ratio of 4.2 at 180 °C after two different incubation times. The growth velocities between 4 and 6 nm/s hold for an incubation time of 2 min and in-between 10 and 11 nm/s for an incubation time of 10 min.

These results show that during heating (and simultaneous electron-beam exposure) "relaxations" within the films take place, which enable a subsequent faster growth. Instead of relaxations, a still slowly increasing temperature (with a few degrees) may be a more obvious explanation for the present observations. However, there are clear indications, as will be explained below, that this more obvious explanation does not hold. The word relaxation implies that the physical picture behind the mechanism that leads to an increased growth rate is understood (such as stress or structural relaxations), but this is not the case. The word relaxation is adopted since it was used to explain very similar behavior observed in previous work on as-sputter-deposited amorphous $Sb_{0.87}Ge_{0.13}$ films.[12] This article reported that local relaxations produced by laser irradiation resulted in a decrease of crystallization temperatures, an increase of crystal-growth velocity and a lowering of the activation energy for growth. In the previous work, it was not observed (at least not mentioned) that due to heating and/or electron irradiation the as-deposited film showed corresponding relaxation phenomena as observed with local laser irradiation. This is a new finding of the present work for phase-change films.

These relaxations are pronounced for the presently studied sputtered films and therefore easy to detect but were not detected in our previous study on electron-beam evaporated phase-change films.[5] Possible origins for the relaxations in the present films are (i) the clearly larger residual stresses and (ii) the presence of argon within the sputtered film. In this context, it has to be mentioned that also the dielectric layers can have some additional influence. In our previous study the phase change layer was directly evaporated on the Si-nitride membrane, whereas

in the present work they are also sandwiched between thin dielectric layers and the Si-nitride is thicker (25 instead of 10 nm). Therefore the relaxations (of stresses or the release of Ar from the film) within the present phase-change films are more constrained here, maybe do not occur very quickly, and are therefore more apparent.

Results showing that the increasing growth rates are not an artifact caused by a still increasing temperature, but are related to the relaxations, are now given. These results also show that the relaxations can occur fully due to thermal annealing and do not need electron-beam exposure. Figure 4(a) shows crystallization at 170 °C, for a sample that was not previously heated, and Fig. 4(b) shows it for another area of the same sample after it had subsequently been heated for 2 h at 160 °C and 9 min at 180 °C. Note that the second heating the temperature is also approached from below, identical to the first heating. The second heating at 170 °C showed a shorter incubation time. According to the results shown in Fig. 3, this would mean a lower growth velocity. However, in Fig. 3, the difference in incubation time is just a difference in statistical probability that crystallization starts in a certain area (where all areas have identical history). In Fig. 4 the incubation time will on average be clearly shorter the second time at 170 °C than the first time due to the annealing that took place in the mean time (because areas have different thermal histories). Moreover, due to this annealing, the film was more "relaxed," allowing a higher growth velocity. This increase in growth velocity apparently outweighed the decrease in incubation time. Note that this effect, shown in Fig. 4, has been observed several times.

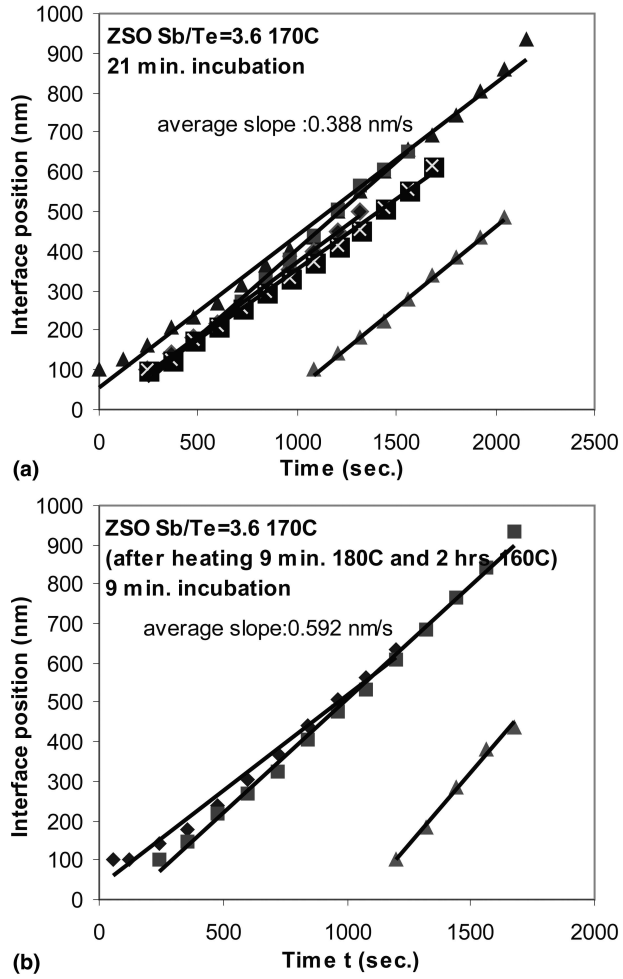

FIG. 4. Interface positions (corrected for drift) as a function of time during crystallization of a film with an Sb/Te ratio of 3.6 at 170 °C after two different annealing conditions. In (a) the film is not annealed previously, whereas in (b) the film is annealed 2 h at 160 °C and 9 min at 180 °C before the crystal growth is measured.

Further important proof comes from recent in situ TEM measurements in which during crystal growth at elevated temperatures, electron irradiation was excluded.[7] Heating is performed during fixed time intervals, and between each interval, the sizes of growing crystallites are recorded, after cooling, at room temperature. These measurements also show that the growth velocity increases with time, and when this method is used, it is impossible that this increase is an artifact due to a still increasing temperature during the course of growth. Further, these recent measurements were performed on phase-change films sputtered from a single target. This also excludes the possibility that due to the use of multiple targets during sputtering in the present work, the film is not fully homogeneous and therefore would show the presently observed relaxations. More work is needed to understand the relaxation phenomenon observed in Ref. 12 and here, but its existence is clear.

C. Crystal growth velocities influenced by the Sb/Te ratio and dielectric-layer type

The main results of the present work are shown in Fig. 5. The measured crystal growth velocities for the various Sb/Te ratios and the two types of dielectric layers are plotted as a function of transformation temperature. The plot is Arrhenius type, i.e., showing the logarithm of the crystal growth velocity as a function of reciprocal temperature. The slopes of the linear regressions in Fig. 5 allow the assessment of the activation energy for growth. Note that one additional data point, holding for $x = 3.0$ and ZSO at 190 °C, is shown in Fig. 5 but is not included in the linear fit because it did not fulfill the requirement of absence of crystallization before the desired isothermal transformation temperatures is reached (see Sec. III. A). Most data points shown in Fig. 5 are an average of about 5 separately measured interface velocities. Accordingly error bars can be added to Fig. 5, but they are not shown, because they cannot be distinguished properly due to overlap, and instead of providing more information, Fig. 5 becomes less clear. Standard

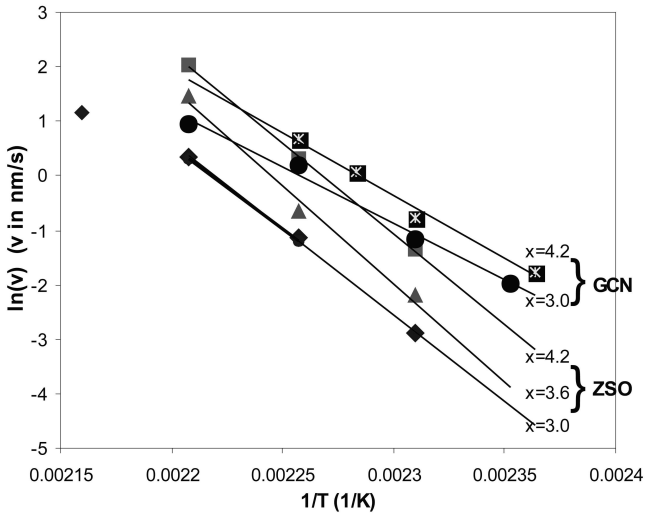

FIG. 5. Logarithm of the crystal growth velocity versus the reciprocal temperature for the various Sb/Te ratios x and the two types of dielectric layers (ZnS–SiO_2 or GeCrN).

deviations in growth velocity range from ±10% to ±100%. Despite the large influence of the relaxations, which make an accurate determination (without systematic errors) of the crystal growth rate difficult, the differences between the various Sb/Te ratios and the two dielectric layers are so pronounced that important conclusions can still be drawn: (i) When the dielectric layers are of type ZSO, the crystal-growth velocity within the Sb/Te = 4.2 films is about 5 times higher than within the Sb/Te = 3.0 ones. For Sb/Te = 3.6, the growth velocity is intermediate. (ii) When the dielectric layers are of type GCN, the crystal-growth velocity within the Sb/Te = 4.2 films is about 2 times higher than within the Sb/Te = 3.0 ones. (iii) The activation energy for growth is not significantly dependent on the Sb/Te ratio but is clearly different for growth between the two types of dielectric layers. The activation energy for growth is on average about 2.9 eV in the case of ZSO and about 2.0 eV in the case of GCN; a difference of nearly 50% exists. (iv) For the temperature interval considered, the growth rate within phase-change films with the same composition is generally higher if the dielectric layers are of type GCN. However, since the activation energy for growth is clearly higher in case of ZSO, this distinction will reverse at higher temperatures. The transition for this reversal for Sb/Te = 4.2 already occurs around 175 °C and for Sb/Te = 3.0 around 190 °C. (v) The incubation time for crystallization is longer in case of ZSO than GCN. (vi) A tentative conclusion is that a higher Sb/Te ratio leads to a slightly longer incubation time.

In our previous study on Sb_xTe films, we found an activation energy of 1.6 eV for the undoped film and about 2.4 eV in case of 5 at.% Ge addition.[5] The present films contain about 8 at.% dopants (but with In, that increases the activation energy less than it does with Ge) and are thus expected similar to the second type of film in the previous study. However, these previous films were not sandwiched between dielectric layers. Therefore, it is intriguing that for ZSO, the activation energy for growth is about 0.5 eV higher and for GCN about 0.5 eV lower than the previous result of 2.4 eV. The former result fits excellently with earlier work, where the activation energy for the overall crystallization process was determined, showing that capping with ZSO leads to an increase of the activation energy with 0.4 to 0.5 eV.[13,14] (Note that this direct comparison between the activation energy for growth and the overall activation energy can be made, as explained in the last sentence of this section.)

Other growth studies show activation energies of 1.6 eV (Si_3N_4 sandwich, but data show a lot of scatter)[9] and 2.4 eV (on SiO_2)[10] for $Ge_2Sb_2Te_5$, 2.35 eV for $Ge_2Sb_2Te_5$ [on Si(100)],[11] 2.74 eV for Ge_4SbTe_5 [on Si(100)],[11] and 2.90 eV for $Ag_{5.5}In_{6.5}Sb_{59}Te_{29}$ [on Si(100)].[11] The composition of the films used to obtain this last result is most comparable to the present ones (i.e., has most comparable Sb/Te ratio and a similar dopant level), and the result is also the same as obtained in case of dielectric layer type ZSO. The crystal shapes and sizes observed for $Ag_{5.5}In_{6.5}Sb_{59}Te_{29}$ with atomic force microscopy (AFM)[11] are also comparable with the results obtained here. However, an important difference is that in Ref. 11, only growth of pre-existing nuclei was observed (so all crystals have at each instance a similar size), whereas in the present work, although nucleation is also dominant at the beginning of crystallization, nuclei still develop during later stages of the transformation (compare Figs. 6 and 7). This results here in a broader crystal-size distribution. In both cases, nucleation is (expected to be) heterogeneous at the film surface (influence of native oxide?) in Ref. 11 and at the interface between the phase-change and the dielectric layers in the present work.

Apart from the above-mentioned activation energies for growth, a larger number of activation energies for the overall crystallization of phase-change films ($Ge_2Sb_2Te_5$) were determined. Also for the overall activation energy Q, similar values in the range from 2 to 3 eV were obtained; see e.g., Refs. 9, 13, and 14. This is not surprising, because mostly these activation energies are related to the activation energies for nucleation E_n and growth E_g separately according to[15]

$$Q = \frac{E_n + dmE_g}{1 + dm} \quad , \tag{1}$$

where d is the dimensionality of growth, which for crystallization in the phase change films is 3 or 2 depending on the crystal size versus the film thickness, and m is the growth mode with $m = 1$ when the position of the growth front (the advancement of the interface) is a linear

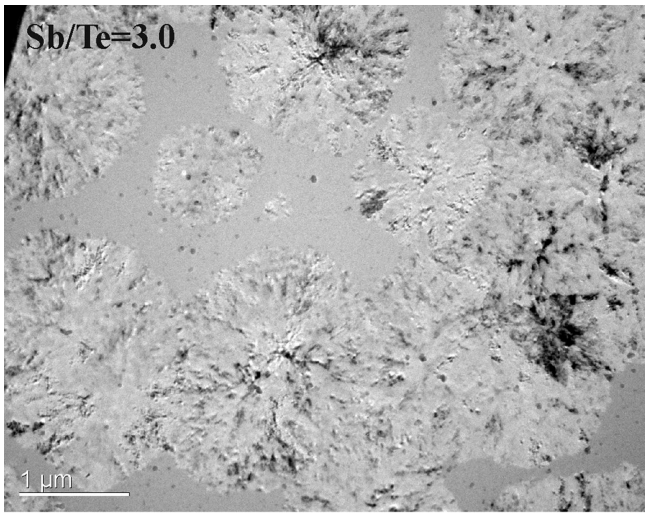

(a)

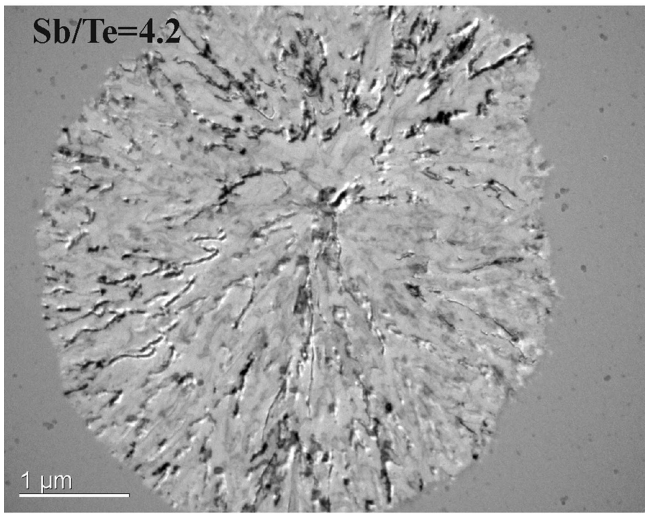

(b)

FIG. 6. After crystallization at 170 °C, a grain size of 1.5–2 μm develops within the films with an Sb/Te ratio 3.0 as shown in (a) and a grain size of about 6 μm within the films with an Sb/Te ratio 4.2 as shown in (b). In both cases the phase-change layer was sandwiched between ZnS–SiO_2.

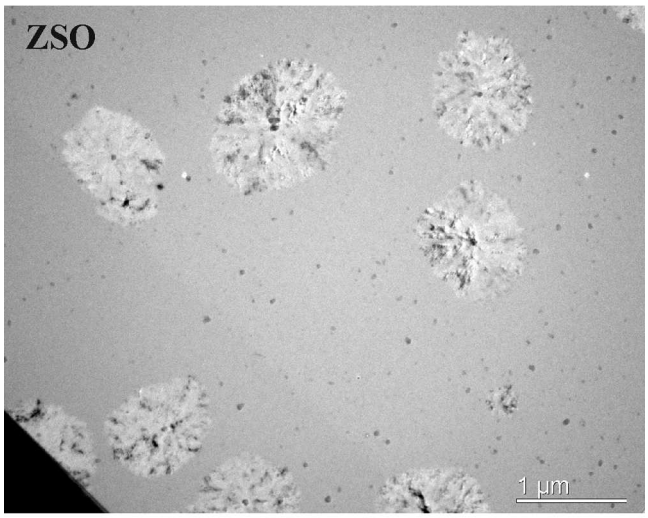

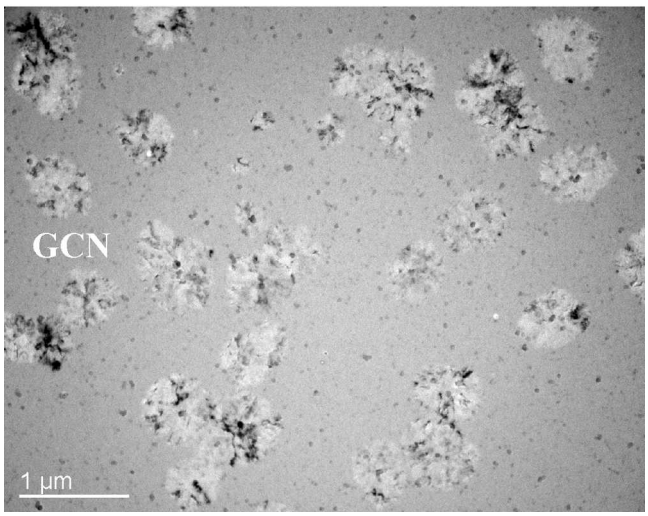

FIG. 7. Despite a growth rate that is a factor 3.5 to 4 higher at 170 °C when GeCrN is used instead of ZnS–SiO_2, the grain size after crystallization attains a value that is a factor 2 smaller, pointing at a clearly higher nucleation rate in case of GeCrN. In both cases the Sb/Te ratio of the films was 3.0.

function of time (i.e., when a constant growth velocity holds e.g. in case of interface-controlled growth) and $m = 1/2$ when its position depends on the square root of time (e.g. in case of diffusion-controlled growth). Note that in this last case, Eq. (1) is approximate. The denominator in Eq. (1) is identical to the transformation index or the so-called Avrami exponent known from the Johnson–Mehl–Avrami–Kolmogorov theory. In phase-change films, due to the fast crystallization rates needed, diffusion-controlled growth is avoided, and m should thus have a value of 1. Classical nucleation theory states that E_n is higher than E_g, but for easy heterogeneous nucleation the difference between E_n and E_g becomes very small, indicating that Q becomes nearly the same as E_g.

D. Nucleation rates influenced by the Sb/Te ratio and dielectric-layer type

Although direct measurements of the nucleation rate were not performed in the present work, an analysis (at room temperature) of the colony size and its distribution (developed at elevated temperature) still enable useful information on the nucleation rate to be obtained. Figure 6 shows images with identical scales of crystals formed at 170 °C in the films with $x = 3.0$ and $x = 4.2$ sandwiched between ZSO. It is clear that the grain size is several times larger in case of the faster growing $x = 4.2$ film. Now the question is, if this faster growth together with a constant nucleation rate can explain the difference in average grain size. Based on the theoretical analysis described in Ref. 9, it can be derived relatively easily that the average crystal diameter or radius (during later stages

of the transformation, i.e., fraction transformed larger than 0.5) scales with $(G^a/I_0)^{1/(a+d)}$, where G is the constant growth rate with growth occurring in d dimensions and where the nucleation rate per unit of untransformed area obeys $I = I_0 t^{a-1}$, with t the time and a an exponent for the time dependence of the nucleation rate. Knowing for the present work that $d = 2$ and a is ibetween 1 (i.e., continuous nucleation rate) and 0 (i.e., nucleation rate clearly decreases as a function of time, similar to preexisting nuclei), shows that the average grain size scales with factors between $(G/I_0)^{1/3}$ and $(1/I_0)^{1/2}$, where the latter I_0 can also be regarded as the number of preexisting nuclei per unit of area. The difference in growth rate between the $x = 3.0$ and $x = 4.2$ films is about 5 times, and the difference in crystal diameter is 3–4 times (see Table I). This indicates with the above information that I_0 is between 5.4 to 16 times larger for the $x = 3.0$ than the $x = 4.2$ film. So, to explain the difference in grain size, a decrease in nucleation rate even larger than the increase in growth-rate is needed when changing from $x = 3.0$ to $x = 4.2$.

An example of the influence of the sandwich layer on the nucleation rate is depicted in Fig. 7. Despite a growth rate that is 3.5–4 times faster at 170 °C in the case of GCN than ZSO, the grain size is a factor of 2 smaller. This means that the nucleation rate in case of GCN is between 4 and 32 times faster than it is in case of ZSO. Therefore the difference in nucleation rate is more pronounced than the difference in growth rate here. However, here, both the nucleation and the growth rates increase when going from ZSO to GCN. Note that this difference in nucleation rates is not caused by different densities of nano-clusters, which act as preferential nucleation sites as mentioned in Sec. III. A because these densities were similar for both types of samples.

A strong influence of the type of dielectric layers on the heterogeneous nucleation could of course be anticipated a priori (see also earlier results and discussions on this matter[9,13]). However, the direct measurement of the strong influence of the dielectric layers on the growth rate is a new, less expected and exciting result.

E. Why do the dielectric layers influence the crystal growth rate?

An indirect observation that the dielectric layers affect the growth velocity was recently proposed in Ref. 16 and is based on finding a maximum in the crystallization velocity for a certain phase change film thickness (9 nm in their case). Both thinner and thicker films lead to a clear decrease of the crystallization velocity. Although the theoretical analysis to explain this observation in Ref. 16 is not correct from a fundamental point of view [showing flaws in the interpretation of the activation energy E and the Gibbs-free-energy change upon crystallization ΔG in Eq. (2), used to describe the temperature dependence of the growth velocity], their conclusion that the dielectric layers adjacent to the phase-change layer can directly affect the crystal-growth rate is supported here and is also directly proven by the present results.

To understand this influence, the following equation for the steady state interface velocity υ during a phase transformation based on the flux of atoms in two directions across a barrier, as visualized in Fig. 8(a), is helpful[17]

$$\upsilon = \upsilon_0 \exp\left(-\frac{E}{kT}\right)\left[1 - \exp\left(\frac{\Delta G}{kT}\right)\right] \quad , \qquad (2)$$

where E is the activation energy associated with the barrier. If the transformation is about to proceed and the interface attains its steady state velocity, the difference in

TABLE I. Average crystal diameter, estimated from overview bright-field TEM images as shown in Figs. 6 and 7, after crystallization at 170 °C within the various phase-change layers.

Sb/Te = 3.0 GCN	Sb/Te = 3.0 ZSO	Sb/Te = 3.6 ZSO	Sb/Te = 4.2 ZSO
0.8 ± 0.2 μm	1.7 ± 0.3 μm	4 ± 0.5 μm	6 ± 0.5 μm

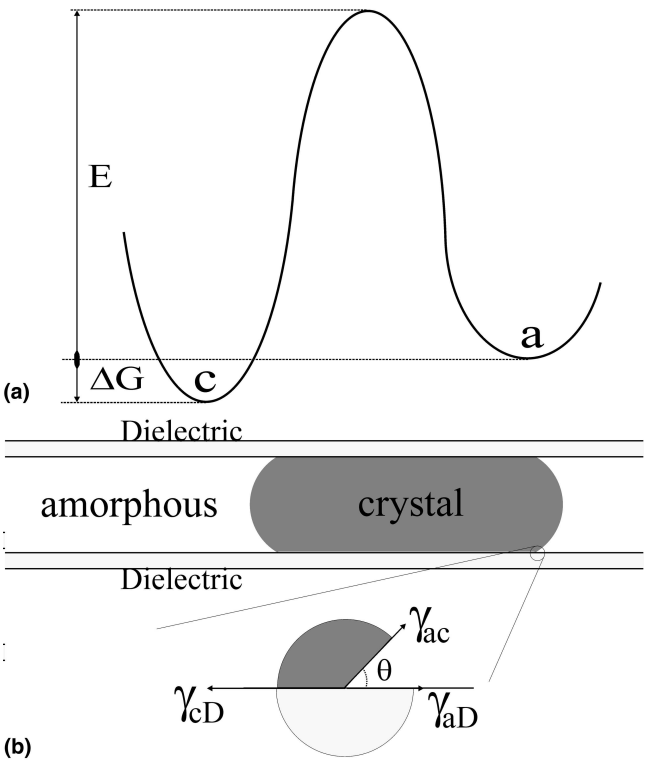

FIG. 8. (a) Schematic representation of the Gibbs-free energy experienced by an atom jumping across the amorphous-crystalline (a-c) interface. (b) During steady-state growth the a-c interface is curved, where the wetting angle of the a-c interface with the adjacent dielectric (D) layers is controlled by the three interfacial energies $\gamma(a\text{-}D)$, $\gamma(a\text{-}c)$, and $\gamma(c\text{-}D)$.

Gibbs-free energy when the atoms jump across the barrier ΔG is smaller than zero. The jump-attempt frequency is taken into account in υ_0. Note that a simplification is made in which all the differences between the two phases across the barrier occur in one atomic step. Knowing that Eq. (2) basically works at the atomic scale, it is also clear that if this atomic scale at the crystalline–amorphous (*c-a*) interface is positioned in the center of the phase change layer or at the interface with the dielectric layers, ΔG, E, and υ_0 are affected. In principle, this means that the crystallization velocity tends to be different in the center of the phase-change layer and at the interfaces with the dielectric layers. This results in a curvature of the *c-a* interface. However, for steady state conditions this curvature and the angle the *c-a* interface makes with respect to the dielectric layers is to large extent controlled by the three interfacial energies γ of the *c-a*, *c-D*, and *a-D* interfaces, as depicted in Fig. 8(b). Since the dielectric films have amorphous structure, $\gamma(c\text{-}D)$ is generally higher than $\gamma(a\text{-}D)$.

Although Eq. (2) works at the atomic scale, ΔG can still be evaluated at a continuum scale. The total change in Gibbs free energy during crystallization is now a summation of the bulk, interfacial, and strain-energy terms. Although strain effects are definitely important for crystallization, it is now sufficient to consider only the bulk and interfacial energy terms

$$\Delta G_{\text{Total}} = (\Delta G_c - \Delta G_a)\pi r^2 d + \gamma_{c-a} 2\pi r d + (\gamma_{c-D} - \gamma_{a-D})\pi r^2 \quad , \tag{3}$$

where r is the radius of the crystal that is considered larger than the thickness of the phase-change film d (compare Fig. 1 where the thickness is only 20 nm and the radius of the order of 100 nm or larger). It is not the purpose of Eq. (3) to use it to determine the critical radius and the corresponding activation energy of a crystal nucleus, because the activation energy E in Eq. (2) and Fig. 8(a) is not equal to the activation energy needed for forming a nucleus with the critical radius. In fact, a steady-state growth velocity of crystals with a size clearly larger than the critical radius has of course not an activation energy E that is related to nucleation; rather E is related to the (local) atomic structure of the *c-a* interface [compare Fig. 8(a)] and is actually the activation energy for growth E_g. Nevertheless, in Ref. 16 it was supposed that in Eq. 2 ΔG is a constant related only to the difference in bulk energies $(\Delta G_c - \Delta G_a)$ and that E is related to activation energy corresponding to a critical nucleus. This is amazing, because in Ref. 16 amorphous marks in fast growth materials were crystallized. In this case, nucleation does not play a role since the crystalline edges just grow to the center of the mark. In principle Eq. (3) shows that the ΔG that must be considered in Eq. (2) is not a constant but depends on, for example, the thickness of the phase-change layer. Since $(\Delta G_c - \Delta G_a) < 0$ and in most cases $(\gamma_{c\text{-}D} - \gamma_{a\text{-}D}) > 0$, it is then clear from Eq. (3) that for decreasing thickness, the growth velocity decreases, and below a certain thickness, crystallization will not occur at all because $\Delta G_{\text{Total}} \geqslant 0$. On the other hand, strain effects, neglected in Eq. (3), become more pronounced for thicker films.[5,8] Therefore, the optimum in crystal-growth velocity observed in Ref. 16 is likely to be an interplay between strain and interfacial effects, where the former and latter explain the decreasing growth velocity above and below a specific thickness (9 nm in Ref. 12), respectively. However, the main point here is not to discuss an optimum in crystal-growth velocity for a specific thickness, but to show that indeed for sufficient thin phase-change layers (here 20 nm) it can be expected that the dielectric layer types directly affect the nucleation rate and the growth rate.

IV. CONCLUSIONS

In situ heating in a TEM in the temperature range 150–190 °C allowed the measurement of the crystal-growth velocity in sputtered phase change films based on three different Sb/Te ratios (3.0, 3.6, and 4.2) and as sandwiched between two types of dielectric layers: ZSO or GCN. During annealing and electron-beam exposure, relaxations within the sputtered films lead to a growth rate that slowly but continuously increases with time. The growth rate within the Sb/Te = 4.2 films is about 5 times higher than that within the Sb/Te = 3.0 films when ZSO is used. With GCN, the crystal-growth velocity within the Sb/Te = 4.2 films is about 2 times higher than within the Sb/Te = 3.0 films. The activation energy for growth is not strongly dependent on the Sb/Te ratio but is clearly different for growth between the two types of dielectric layers. The activation energy for growth is on average about 2.9 eV in the case of ZSO and about 2.0 eV for GCN. For the temperature interval considered, the growth rate within phase-change films with the same composition is generally higher if the dielectric layers are of type GCN, but this reverses after a relatively small temperature increase due to the higher activation energy for growth in the case of ZSO. The incubation time for crystallization is longer if ZSO is used instead of GCN. The average grain size after crystallization indicates that the nucleation rate decreases more strongly than the growth rate increases when the Sb/Te ratio is changed from 3.0 to 4.2 (in the case of ZSO) and that the nucleation rate increases more strongly than the growth rate increases when changing from ZSO to GCN (for an Sb/Te ratio of 3.0).

REFERENCES

1. T. Ohta, N. Yamada, H. Yamamoto, T. Mitsuyu, T. Kozaki, J. Qiu, K. Hirao: Progress of the phase-change optical disk

memory, in *Applications of Ferromagnetic and Optical Materials, Storage and Magnetoelectronics*, edited by H.J. Borg, K. Bussmann, W.F. Egelhoff, Jr., L. Hesselink, S.A. Majetich, E.S. Murdock, B.J.H. Stadler, M. Vázquez, M. Wuttig, and J.Q. Xiao (Mater. Res. Soc. Symp. Proc. **674**, Warrendale, PA, 2001), V1.1.
2. G-F. Zhou: Materials aspects in phase change optical recording. *Mater. Sci. Eng.* **A304–306,** 73 (2001).
3. H. Borg, M. Lankhorst, E. Meinders, W. Leibrandt: Phase-change media for high-density optical recording, in *Applications of Ferromagnetic and Optical Materials, Storage and Magnetoelectronics*, edited by H.J. Borg, K. Bussmann, W.F. Egelhoff, Jr., L. Hesselink, S.A. Majetich, E.S. Murdock, B.J.H. Stadler, M. Vázquez, M. Wuttig, and J.Q. Xiao (Mater. Res. Soc. Symp. Proc. **674,** Warrendale, PA, 2001), V1.2.
4. H.J. Borg, P.W.M. Blom, B.J.A. Jacobs, B. Tieke, A.E. Wilson, I.P.D. Ubbens, and G. Zhou: AgInSbTe materials for high speed phase-change recording. *Proc. SPIE* **3864,** 191 (1999).
5. B.J. Kooi and J.Th.M. De Hosson: On the crystallization of thin films composed of $Sb_{3.6}Te$ with Ge for rewritable data storage. *J. Appl. Phys.* **95,** 4714 (2004).
6. B.J. Kooi, W.M.G. Groot, and J.Th.M. De Hosson: In-situ transmission electron microcopy study of the crystallization of $Ge_2Sb_2Te_5$. *J. Appl. Phys.* **95,** 924 (2004).
7. R. Pandian, B.J. Kooi, J.Th.M. De Hosson, A. Pauza (unpublished).
8. V.Yu. Kolosov and A.R. Thölen: Transmission electron microcopy studies of the specific structure of crystals formed by phase transition in iron oxide amorphous films. *Acta Mater.* **48,** 1829 (2000).
9. G. Ruitenberg, A.K. Petford-Long, and R.C. Doole: Determination of the isothermal nucleation and growth parameters for the crystallization of thin $Ge_2Sb_2Te_5$ films. *J. Appl. Phys.* **92,** 3116 (2002).
10. S. Privitera, C. Bongiorno, E. Rimini, R. Zonca, A. Prirovano, and R. Bez: Amorphous-to-polycrystal transition in GeSbTe thin films, in *Advanced Data Storage Materials and Characteriztion Techniques*, edited by J.W. Ahner, J. Levy, L. Hesselink, and A. Mijiritskii (Mater. Res. Soc. Symp. Proc. **803,** Warrendale, PA, 2004), HH1.4, p. 83.
11. J. Kalb, F. Spaepen, and M. Wuttig: Atomic force microscopy measurements of crystal nucleation and growth rates in thin films of amorphous Te alloys. *Appl. Phys. Lett.* **84,** 5240 (2004).
12. M.C. Morilla, C.N. Afonso, A.K. Petford-Long, and R.C. Doole: Influence of the relaxation state on the crystallization kinetics of Sb-rich SbGe amorphous films. *Philos. Mag. A* **73,** 1237 (1996).
13. N. Ohshima: Crystallization of germanium-antimony-tellurium amorphous thin film sandwiched between various dielectric layers. *J. Appl. Phys.* **79,** 8357 (1996).
14. I. Friedrich, V. Weidenhof, W. Njoroge, P. Franz, and M. Wuttig: Structural transformations of $Ge_2Sb_2Te_5$ films studied by electrical resistance measurements. *J. Appl. Phys.* **87,** 4130 (2000).
15. B.J. Kooi: Monte Carlo simulations of phase transformations caused by nucleation and subsequent anisotropic growth: Extension of the Johnson–Mehl–Avrami–Kolmogorov theory. *Phys. Rev. B* **70,** 224108 (2004).
16. H.C.F. Martens, R. Vlutters, and J.C. Prangsma: Thickness dependent crystallization speed in thin phase change layers for optical recording. *J. Appl. Phys.* **95,** 3977 (2004).
17. D.A. Porter and K.E. Easterling: *Phase Transformations in Metals and Alloys* (Van Nostrand Reinhold Company, New York, 1981), pp. 132–136.